

DIRECT THERMAL-TO-ELECTROCHEMICAL ENERGY CONVERSION VIA A PYROELECTROCHEMICAL CELL

Tim Kowalchik¹, Fariha Khan², Shad Roundy¹ and Roseanne Warren¹

¹Department of Mechanical Engineering, University of Utah, Salt Lake, UT, USA

²Department of Electrical and Computer Engineering, University of Utah, Salt Lake, UT, USA

ABSTRACT

This work demonstrates a novel concept for the *direct conversion* of thermal energy to stored electrochemical energy that the authors call a “pyroelectrochemical cell” (PEC). The PEC uses a porous pyroelectric material as the separator of supercapacitor. Thermal energy (in the form of a temperature change with time) generates a voltage across the separator, which induces ion migration and charges the cell. Experimental results validate the device concept by demonstrating the separator’s dual functionality as pyroelectric material and porous membrane. A PEC with pyroactive separator was held at 50 mV and heated from 20 to 30°C at a rate of 0.336 °C/min. When the separator pyroelectric field is oriented with positive dipole at the anode, chronoamperometric current increases by 155% due to heating, generating 9.66 mJ over the one-hour test. In a separate heating test (50 mV, 20 to 55 °C), when the separator orientation is reversed, changing the direction of the heating induced electric field, chronoamperometric current decreases from 15.3 μ A to 5.2 μ A, indicating the expected directional response of the pyroelectric separator.

KEYWORDS

Pyroelectricity. Supercapacitor. Energy harvesting. Porous thin films. Electrochemical cell.

INTRODUCTION

Ambient thermal energy is an abundant resource that can be harvested to power wireless sensors and internet-of-things (IoT) devices. IoT information systems have transformative potential in industrial applications, precision agricultural, and wearable health sensors [1]. Developing innovative methods of powering such devices, e.g. by wireless power transfer or ambient energy harvesting, is critical to creating real-world systems capable of self-sufficient operation [2]. Pyroelectric materials harvest ambient thermal energy in the form of temperature fluctuations with time (dT/dt). This work explores a new concept for *direct integration of pyroelectric and supercapacitor materials at the cell level* that may function as a “self-charging” pyroelectrochemical cell (PEC) for low-power (*i.e.* 10’s-100’s μ W) IoT sensors.

Figure 1 provides a conceptual illustration of the PEC. The cell is an electrochemical double layer capacitor, composed of two symmetric electrodes, electrolyte, and a porous, pyroelectric separator. The pyroelectric separator used in this work is a composite film of polyvinylidene fluoride-barium titanate nanoparticles (PVDF-BT). BT particles increase the pyroelectric response of the film, while the porous PVDF matrix permits ion movement across the separator. When the cell experiences a change in temperature with time, dipoles within the separator rotate and a pyroelectric voltage arises in response to the thermally-induced polarization of the membrane (Figure 1b). The electric field drives ion migration through the porous separator, charging the electrochemical double

layer within the cell (Figure 1c).

The aim of this work is to experimentally validate our theory of PEC device physics by exploring the chronoamperometric response of cells to controlled heating and cooling cycles (dT/dt). Chronoamperometry experiments are conducted on PEC devices with different PVDF-BT separator orientations with respect to the cell cathode/anode, as well as on control cells with unpoled PVDF-BT and Celgard separators. Evidence of an orientation-dependent effect on PEC response to a temperature change supports the theory of PEC functionality presented in Figure 1. Additionally, the present work aims to distinguish thermal effects from pyroelectric effects occurring in the PEC. Thermal effects are defined as those resulting from pure cell heating (or cooling) of a non-pyroelectric supercapacitor, while pyroelectric effects are those resulting directly from the changing electric field of the separator.

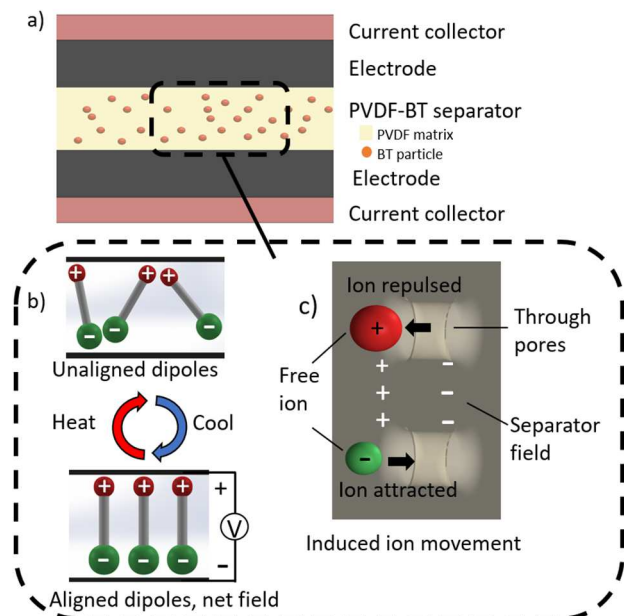


Figure 1: PEC CONCEPT AND FUNCTION. a) A representative PEC device is composed of symmetric supercapacitor electrodes and a pyroactive porous separator. b) Upon heating or cooling ($dT/dt \geq 0$), dipoles in the separator change alignment, generating a voltage across the separator and c) charging the supercapacitor via electric field-driven ion movement.

METHODS

Porous, pyroelectric PVDF-BT films were fabricated by coagulation bath method and corona poling, as described in previous works [3,4]. PVDF powder (average MW \sim 534,000 g/mol) was dissolved in N,N-dimethylformamide (DMF) at 12% w/w in a 45°C water bath; BT particles (BaTiO_3 , Stanford Advanced Materials, 150 nm particle size) were dissolved in DMF to produce a final PVDF:DMF ratio of 15% w/w upon mixing. PVDF-BT suspensions (80:20 w/w) were drop-cast onto a glass

slide and the films submerged in a deionized (DI) water bath for 20 minutes to produce a porous structure. The films were dried at 60°C in an oven, then annealed for 5 hours at 90°C (“unpoled films”). Corona poling was applied at 5 kV/cm for 24 hours to create pyroactive films (“poled films”). Film porosity was measured by dry-wet weight method using butanol as the wetting liquid [5]. Pore structure was examined through scanning electron microscopy (SEM) of film cross sections. Pyroelectric coefficient was measured using metalized PVDF-BT films. Films were metalized by sputtering 10 nm Ti and 50 nm Au. Films were heated by an infrared bulb for 15 s at 0.67 °C/s. Film temperature and pyroelectric voltage response were measured using a thermocouple and voltage-follower circuit, respectively.

Supercapacitor cells were assembled using symmetric graphite on copper electrodes (MTI Corp) for both the cathode and anode, 0.5 M Na₂SO₄ electrolyte, and one of the following separators: i) a commercial separator (Celgard 2340), ii) unpoled PVDF-BT film, or iii) poled PVDF-BT film. Cells were assembled using a custom set-up that enables constant temperature or dT/dt rate control by immersion in a temperature-controlled water bath. Electrochemical testing of cells was conducted using a Gamry reference 600+ potentiostat. Cyclic voltammetry (CV) (50 cycles, 100 mV/s) and electrochemical impedance spectroscopy (EIS) were conducted at 20 °C and 30 °C constant cell temperature. All cells were cycled *via* CV for 20 minutes before chronoamperometry measurements to ensure cell stability prior to thermal testing. CV and EIS were also done post-chronoamperometry to characterize changes to cell properties over the course of testing.

Chronoamperometry measurements were conducted at 50 mV constant applied potential while the cells were heated and/or cooled at a controlled rate (dT/dt). Cells were tested over four temperature ranges for heat/cool cycles: i) 20 °C to 10 °C (cool, then heat), ii) 20 °C to 30 °C, iii) 20 °C to 40 °C, and iv) 20 °C to 55 °C (heat, then cool for ii-iv). Cells were rested for 20 minutes between tests, with the electrodes shorted to allow discharging. The “baseline” current required to maintain 50 mV was measured for each cell for 15 minutes before thermal testing. Chronoamperometry measurements between different cells during thermal cycling are reported as “normalized” currents, where the current measured during heating or cooling experiments was divided by the baseline current for a given cell. This approach enables comparison of dT/dt responses among cells with control (Celgard), unpoled PVDF-BT, and poled PVDF-BT separators, which have varying baseline chronoamperometric current as a result of different separator compositions. To test the directionality of the pyroelectric response in a given cell, cell wiring was disconnected and flipped after each thermal cycle to reverse the orientation of the separator with respect to the cell cathode/anode. For these orientation comparisons, reported current was zeroed to the baseline chronoamperometric current for each test. PEC energy conversion was calculated from chronoamperometry measurements using Equation 1:

$$E = V * \int_{t_1}^{t_2} I(t) dt \quad (1)$$

where E is energy, V is the constant voltage applied, I is

current, and t_2-t_1 is the time elapsed during heating.

Pyroelectric orientation was also investigated through an open circuit potential (OCP) measurement under more rapid heating conditions (13.8 °C/min for 15 s). The cell was cooled to return to room temperature over 20 minutes after each test.

RESULTS

PVDF-BT Separator

PVDF-BT separator films have an average thickness of $60 \pm 5 \mu\text{m}$ and average porosity of $62 \pm 2\%$. The separator porosity consists of a larger “finger-like” through-pores and smaller pores distributed throughout the film cross-section (Figure 2). The average width of the finger-like pores, as determined from measurements of SEM images, is $8.50 \pm 1.10 \mu\text{m}$; smaller circular pores within these structures have $0.82 \pm 0.13 \mu\text{m}$ average diameter.

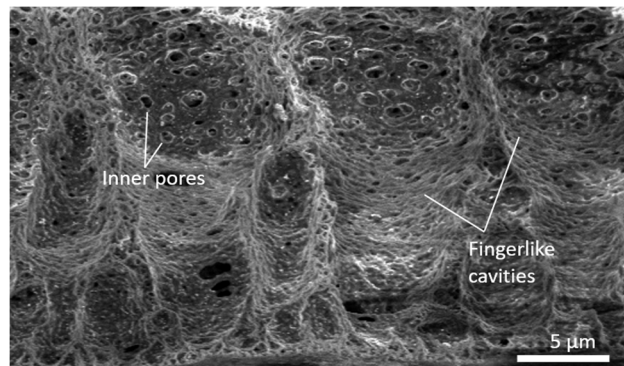


Figure 2: PVDF-BT STRUCTURE. Cross-sectional SEM image of the PVDF-BT separator. The PVDF matrix is composed of two types of pores: larger finger-like cavities through the film thickness and smaller pores spread throughout the matrix.

Once poled, the PVDF-BT separator has a pyroelectric coefficient of $59 \pm 2 \mu\text{C/m}^2\text{K}$, and produces a pyroelectric voltage of 100 mV when heated at a rate of 0.67 °C/s (Figure 3). Repeated testing of the same sample showed no decrease in pyroactivity over the course of one week. All PEC testing was conducted within one week of poling to ensure the pyroactivity of the separators remained consistent during testing.

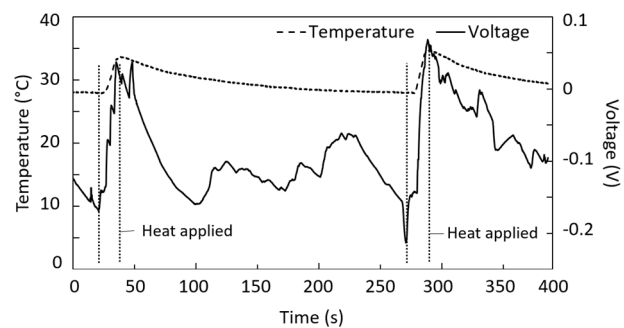


Figure 3: PYROELECTRIC FUNCTION. Experimental validation of porous PVDF-BT film pyroelectric response.

Electrochemical Cell Function

The electrochemical separator functionality of porous PVDF-BT films was evaluated by CV and EIS measurements of symmetric, two-electrode supercapacitor cells using unpoled PVDF-BT separators (Figure 4).

Equivalent series resistance values extrapolated from EIS measurements indicate low overall cell resistance in supercapacitors constructed with PVDF-BT films (Figure 4a). Cell temperature has a negligible effect on equivalent series resistance over the range of temperatures tested (15.6 Ω at 20°C; 16.1 Ω at 30°C).

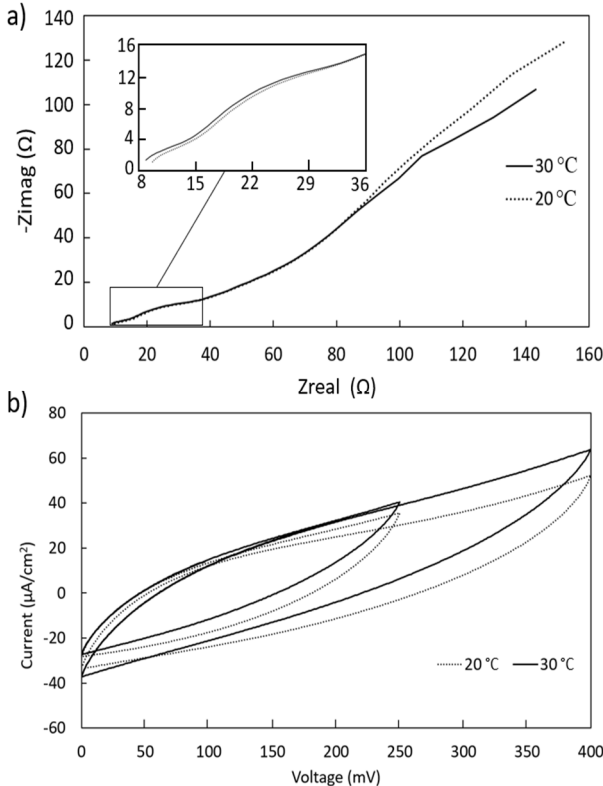


Figure 4: PEC CV AND EIS RESULTS. a) EIS measurements of a PEC with unpoled PVDF-BT separator at 20 °C and 30 °C. b) CV measurements of the same PEC at 20 °C and 30 °C show capacitive behavior characteristic of electrochemical double layer capacitors, indicating good ion flow across the separator and the expected charging function.

CV measurements of the PEC display the expected shape for an electrochemical double layer capacitor, indicating that the PVDF-BT separator allows ion movement within the cell (Figure 4b). As expected, there is a moderate increase in cell capacitance when cell temperature increases. Increasing cell temperature changes numerous properties, including double layer thickness, and electrolyte ionic conductivity [6]. The combined changes within a cell result in an increase in capacitance with temperature. From 20 °C to 30 °C the capacitance increased from 3.48 mF to 3.97 mF (1.14x) over the 250 mV scan range, and from 4.34 mF to 5.17 mF (1.19x) over the 400 mV scan range. No reaction peaks were observed over these scan ranges, which exceed the cell voltage ranges used during pyroelectric testing. CV measurements are unaffected by the PVDF-BT separator being poled vs. unpoled.

Control Cell vs PEC Thermal Cycling

Direct conversion of thermal energy to stored electrochemical energy was demonstrated via chronoamperometry measurements a PEC devices. Cells

were held at 50 mV potential, and heated and cooled at 0.336 °C/min. The separator was oriented such that the pyroelectric-induced electric field would aid ion migration within the cell (Figure 5a). The heating/cooling-induced charging current was measured and compared to the non-pyroactive control (Celgard separator). The control cell shows a peak normalized increase in current of 35% over the baseline current during the 20 minute heating step (Figure 5b), converting 2.51 mJ of thermal energy to stored electrochemical energy. The PEC shows a current increase of 155% during the 20 minute heating step, which corresponds to 9.66 mJ of stored electrochemical energy (8.05 μW average power). The larger energy conversion of the active PVDF-BT cell represents the additional energy converted by pyroelectricity over the thermal response of the Celgard control separator.

During cooling the control cell returns to baseline current as the temperature returns to 20 °C. The increase in current was due to reversible thermal effects, and should/does track the temperature closely. For the PVDF-BT cell, normalized current remained at 1.4x the baseline current when the cell returned to 20 °C. Chronoamperometric current eventually returns to the baseline value, however the time delay relative to the control indicates additional stored energy in the PEC. This suggests the pyroelectric response is adding energy to the supercapacitor electrochemical double layer.

Pyroelectric Orientation Effect

The pyroelectric response of the separator has a directionality based on the orientation of the separator in the cell. Oriented one way, the pyroelectric response of the separator should drive negative ions away from the anode during heating. This is shown as side 1 in Figure 6a. Oriented the opposite way, the negative ions will be attracted to the anode (side 2 in Figure 6a). In reality, there is a baseline thermal response to the cell independent of the pyroelectric response (Figure 5). Thus, the pyroelectric response can either add to or subtract from the thermal response of the cell depending on orientation. For this work, side 1 was defined as the orientation that helped charge the double layer. To investigate directionality of the pyroelectric response, cells with unpoled separators and cells with poled separators in side 1 and side 2 orientations were subject to a 20 to 55 °C thermal cycle chronoamperometry test. Figure 6b shows the cell behavior resulting from flipping the PVDF-BT separator orientation. The unpoled PEC has a peak thermal response of 11 μA . Side 1 of the poled PEC has a peak response of 15.3 μA , and side 2 has a peak of 5.2 μA . The separator appears to be adding to, or subtracting from, the base thermal response of the cell depending on PVDF-BT separator orientation. These results suggest the potential of a PEC to be self-charging when exposed to an environmental thermal cycle. Further experiments are needed to confirm the phenomena, including testing with additional cell compositions, heating rates, and temperature ranges.

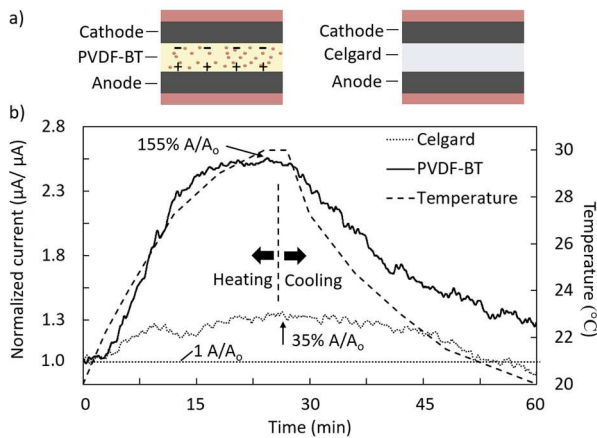


Figure 5: CELL RESPONSE TO HEATING AND COOLING. a) Cross-sectional schematic of cells containing pyroactive PVDF-BT separator and non-active Celgard. b) Normalized current (current/baseline) is shown and the peak normalized current is labeled for both cells. Pyroactive PVDF-BT shows a peak current increase of 155% vs 35% for the Celgard control.

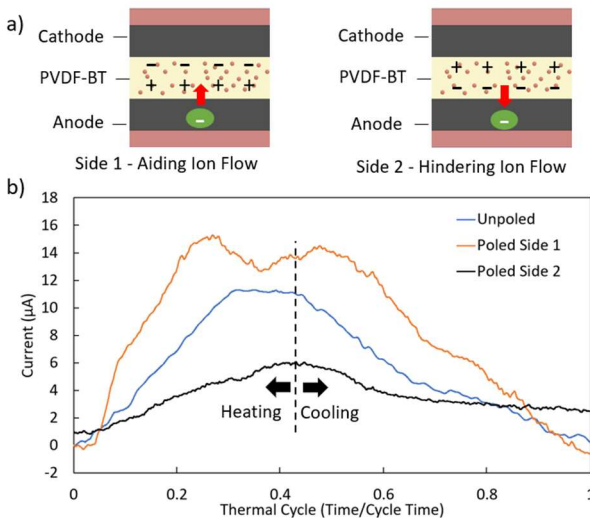


Figure 6: EFFECT OF SEPARATOR ORIENTATION ON CHRONOAMPEROMETRY. a) Schematic of side 1 vs. side 2 orientation. b) Cell current response to a 20-55 °C (0.774 °C/min) heating, then cooling, cycle while holding the cathode at a constant 50 mV potential. The unpoled current change is 11 μA, side 1 current change is 15.3 μA, and side 2 current change is 5.2 μA.

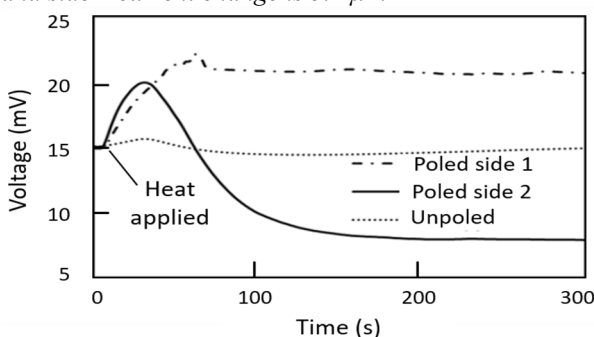


Figure 7: EFFECT OF SEPARATOR ORIENTATION ON OPEN CIRCUIT POTENTIAL. OCP measurements during rapid (13.8 °C/min) heating. Side 1 shows an open circuit potential change of 12 mV from the baseline, side 2 shows a decrease of 13 mV.

As an additional check on pyroelectric directionality, cells with a poled separator and a Celgard control were rapidly heated while measuring OCP (Figure 7). The control returned to baseline OCP within 5 minutes of the heating impulse. The overshoot and subsequent decrease in OCP upon heating of the pyroactive separator (side 2 orientation) is believed to be a response to the sudden pyroelectric current generation. Side 1 OCP increased by 7 mV before stabilizing at 6 mV increase in OCP. Side 2 initially increased by 5 mV, before stabilizing at net 6 mV decrease in OCP. These results further suggest separator orientation-dependence of PEC charging response.

CONCLUSION

This work has demonstrated initial results that provide evidence for a pyroelectrically-driven self-charging supercapacitor. The PVDF-BT separator was shown to be pyroelectrically active and allowed ion flow. Comparing the PEC to a non-pyroactive control showed a 3.8x increase in stored electrochemical energy within the cell upon heating. As expected with pyroelectrically-driven charging, PEC response to heating was directionally dependent on separator orientation.

The next phase of this research will investigate PEC device physics through finite element, as well as continued experimental testing to further characterize PEC behavior.

ACKNOWLEDGEMENTS

The authors would like to thank the Utah Nanofab for the use of their facilities and measurement equipment. This work is supported by NSF (Award no. 1936636).

REFERENCES

- [1] Elahi H. et al. Energy harvesting towards self-powered IoT devices. *Energies*, 13(21) (2020) <https://doi.org/10.3390/en13215528>
- [2] Shirvanimoghaddam M. et al. Paving the path to a green and self-powered internet of things. in *IEEE Access*, 7, 94533-94556 (2017)
- [3] Khan F. et al. Stretching-induced phase transitions in barium titanate-poly(vinylidene fluoride) flexible composite piezoelectric films. *Scripta Materialia*, 193 (2021) <https://doi.org/10.1016/j.scriptamat.2020.10.036>
- [4] Deshmukh S., Li K. Effect of ethanol composition in water coagulation bath on morphology of PVDF hollow fiber membranes. *J. of Membr. Sci.*, 150(1) (1998) [https://doi.org/10.1016/S03767388\(98\)00196-3](https://doi.org/10.1016/S03767388(98)00196-3)
- [5] Ahmad A. et al. Effect of ethanol concentration in water coagulation bath on pore geometry of PVDF membrane for Membrane Gas Absorption application in CO₂ removal. *Separation and Purification Tech.*, 88(22) (2012), <https://doi.org/10.1016/j.seppur.2011.11.035>
- [6] Xiong G., Arpan K., Fisher T. Influence of Temperature on Supercapacitor Performance. In *Thermal Effects in Supercapacitors*, 71-114 (2015) https://doi.org/10.1007/978-3-319-20242-6_4

CONTACT

*Tim Kowalchik, tim.kowalchik@utah.edu